Available online at www.sciencedirect.com
SCIENCE DIRECT
Cement and Concrete Research 35 (2005) 1503–1509
Cement and Concrete Research

Stress relaxation of foamed high-alumina cement paste

Jong-Shin Huang*, Jin-Yuan Lin, Ming-Jang Jang

Department of Civil Engineering, National Cheng Kung University, Tainan, 70101 Taiwan, R.O.C.

Received 3 March 2004; accepted 19 October 2004

Abstract

A series of stress relaxation tests on foamed high-alumina cement pastes with different relative densities under various temperatures and imposed fixed strains were conducted to study the effects of relative density and imposed strain on the stress relaxation rates of foamed high-alumina cement pastes. At the same time, the activation energy for stress relaxation of foamed high-alumina cement paste was determined from experimental results. Experimental results on the stress relaxation rates of foamed high-alumina cement pastes are also compared to a theoretical expression obtained from a cell-edge relaxation-bending model. Consequently, the microstructural coefficients included in the theoretical expression for describing the stress relaxation rates of foamed high-alumina cement pastes are found. Furthermore, the stress relaxation rates of foamed high-alumina cement pastes can be predicted from the theoretical expression once their relative density and the imposed strain are known.

Keywords: Stress relaxation; Micromechanics; Cement paste

1. Introduction

Sandwich panels with metal or plywood faces and a lightweight foam core are extensively being used as load-bearing components in many engineering lightweight structures. The separation of two stiff strong faces by a lightweight foam core increases the bending resistance of sandwich panels, with a little increase in weight. Cement foam cores are preferably used in building construction because of their excellent thermal insulation, low cost as well as good fire resistance. In building construction, cement foam cores with minimum values of mechanical properties are required to ensure the structural integrity of sandwich panels when they are subjected to external loads. The stiffness and strength of cement foam cores, however, are relatively low due to their high porosity. As a result, sandwich panels with cement foam cores are normally weak at bearing points and in transmitting external loads and thus are difficult to join. In practice, mechanical fastening with rivets and bolts is used for joining sandwich panels [1]. When sandwich panels are joined by fasteners with bearing-type of rivets and bolts, a fixed strain is imposed, and the induced stresses within them will relax gradually. In some cases, a catastrophic failure of sandwich panels occurs due to the stress relaxation of cement foam cores. Therefore, the stress relaxation of cement foam cores needs to be investigated to ensure the structural integrity of sandwich panels.

Foamed materials deform primarily by the elastic bending of solid cell walls when they are loaded at lower temperatures as compared to their melting temperatures. Thus, the mechanical properties of foamed materials can be analyzed theoretically from a cell-edge bending model proposed by Gibson and Ashby [2]. Analytical results suggest that the mechanical properties of foamed materials depend on their relative density, cell geometry and the properties of solid material from which they are made. Experimental results on the elastic moduli and strengths of foamed portland cement paste were first reported by Short and Kinniburgh [3]. They found that the mechanical properties of foamed portland cement paste are mainly affected by their relative density. Meanwhile, the elastic

* Corresponding author. Tel.: +886 6 794 3211; fax: +886 6 2358542.
E-mail address: jshuang@mail.ncku.edu.tw (J.-S. Huang).

0008-8846/$ - see front matter © 2004 Elsevier Ltd. All rights reserved.
doi:10.1016/j.cemconres.2004.10.024

moduli, strengths, mode I and II fracture toughnesses and compressive fatigue of foamed high-alumina cement paste were measured and presented by Huang et al. [4–6]. Again, the measured mechanical properties and fatigue life of foamed high-alumina cement paste depend on their relative density, cell geometry and the material properties of solid alumina cement paste from which they are made. Based on the existing experimental results [3–6], it is known that the measured elastic moduli and strengths of foamed cement paste agree well with the theoretical cell-edge bending model.

When sandwich panels are under relatively higher service temperatures, the stress relaxation of foamed cement cores becomes significant and could lead to a catastrophic failure. Therefore, the stress relaxation rates of foamed cement cores are important and thus should be taken into consideration in a structural design. The stress relaxation of foamed materials was analyzed theoretically by Lin and Huang [7] from a cell-edge relaxation-bending model. Lapsa [8] provided a rheological explanation for the stress relaxation phenomena at early phases of foamed mortar using the Bingham's model. By solving the resulting Bingham's equation, the relaxation for the tensile stresses in cell edges and cell faces during the foaming process can be estimated. The stress relaxation of hardened foamed cement paste, however, has been paid little attention. In the paper, measurements on the stress relaxation rates of foamed high-alumina cement paste will be conducted and then compared to a theoretical expression derived from the cell-edge relaxation-bending model to determine the corresponding stress relaxation parameters.

2. Theoretical expression

The cell-edge relaxation-bending model and ideas proposed by Lin and Huang [7] are employed here to obtain a theoretical expression for describing the stress relaxation rate of foamed cement paste. Fig. 1 schematically illustrates an idealized open-cell foam subjected to a fixed uniform strain ε^*. In the model, the cell length is ℓ and the area of each square cross-section is t^2. It is assumed that the stress relaxation of solid cell edges in the model $\dot{\sigma}_s$ can be described well by the following power law relation:

$$\dot{\sigma}_s = \left(\frac{\varepsilon_s}{\varepsilon_{os}}\right)^{n_s} \dot{\sigma}_{os} = \left(\frac{\varepsilon_s}{\varepsilon_{os}}\right)^{n_s} \alpha_s \exp\left(\frac{-Q_s}{RT}\right) \tag{1}$$

where $\dot{\sigma}_{os}$,α_s, n_s and ε_{os} are the stress relaxation parameters of solid cell edges, Q_s is the activation energy for stress relaxation process, R is the ideal gas constant, T is the absolute temperature, and ε_s is the induced normal strain at individual solid cell edges due to a fixed uniform strain ε^* imposed on the outermost boundary of the open-cell foam.

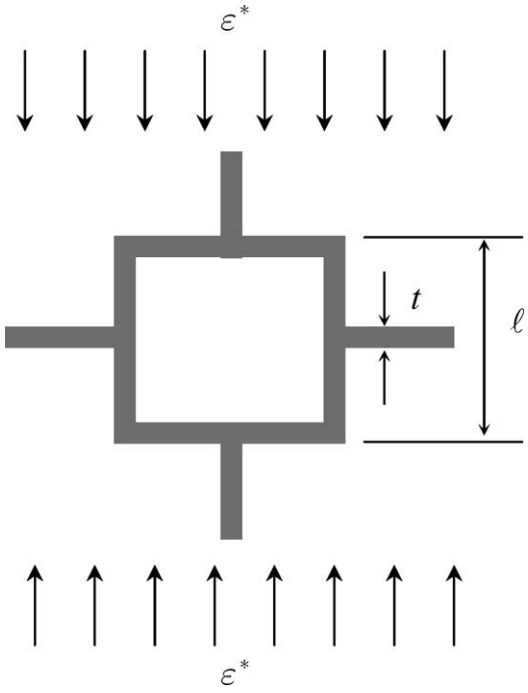

Fig. 1. An idealized open-cell foam with a cell length of ℓ and a cross-sectional area of t^2 subjected to a fixed uniform strain ε^* is schematically illustrated.

When the open-cell foam is under a fixed uniform strain ε^*, the deflection δ of the solid cell edge beam of Fig. 2 is stationary. Then, the induced concentrated force acting at the mid-span of the solid cell edge beam will relax gradually with a steady-state rate of $\dot{F}$. Furthermore, the relaxation rate of external moment exerted on any cross-section of the solid cell edge beam can be calculated from the elementary mechanics of materials. At the same time, the relaxation rate of internal moment acting at any cross-section of the solid cell edge beam can be calculated from equilibrium. Hence, the induced normal strain at any point is related to the curvature of the deformed solid cell edge beam by assuming that plane sections remain plane. For open-cell foams, it is found that $\varepsilon^* \propto \delta/\ell$ and $\dot{\sigma}^* \propto \dot{F}/\ell^2$ by using dimensional argument analysis. As a result of those, the stress relaxation rate of open-cell foams is expressed in terms of their relative density ρ^*/ρ_s [7], defined as the ratio of the density of open-cell foams ρ^* to the density of solid cell edges ρ_s:

$$\dot{\sigma}^* = \frac{1}{C_2 + (2+n_s)} \left(\frac{1+2n_s}{C_1 n_s}\right)^{n_s} \left(\frac{\rho^*}{\rho_s}\right)^{(3+n_s)/2} \times \left(\frac{\varepsilon^*}{\varepsilon_{os}}\right)^{n_s} \alpha_s \exp\left(\frac{-Q_s}{RT}\right) \tag{2}$$

wherein C_1 and C_2 are two microstructural coefficients, depending on the cell geometry of open-cell foams. From Eq. (2), it is found that the stress relaxation rate of open-cell foams depends on their relative density, the imposed strain and the stress relaxation parameters of solid cell edges.

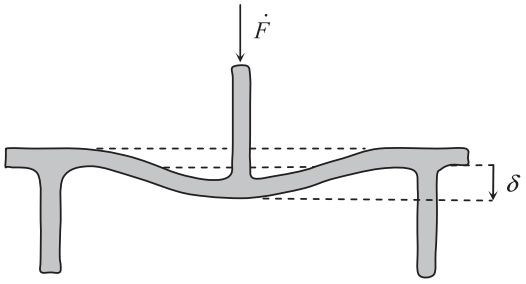

Fig. 2. A solid cell edge beam is employed to analyze the stress relaxation rate of open-cell foams.

When a closed-cell foam, composed of cell edges and cell faces, is subjected to a fixed uniform strain ε^*, the induced bending moment acting at each cell edge produces a bending deflection δ, while the induced normal stress acting at each cell face causes an axial elongation which is proportional to δ. From equilibrium, the total force acting at the closed-cell foam is the sum of the induced force acting at cell edges and the induced force acting at cell faces. Hence, the stress relaxation rate of the closed-cell foam is the sum of the stress relaxation rate of cell edges and that of cell faces. For closed-cell foams, ϕ is defined as the volume fraction of the solid contained in cell edges; in other words, the rest $1-\phi$ is in cell faces. Therefore, the stress relaxation rate of closed-cell foams is found to be [7]:

$$\dot{\sigma}^* = \left[\frac{1}{C_2(n_s+2)}\left(\frac{2n_s+1}{C_1 n_s}\right)^{n_s}\left(\phi\frac{\rho^*}{\rho_s}\right)^{(n_s+3)/2} + \frac{2}{3}(1-\phi)\left(\frac{\rho^*}{\rho_s}\right)\right]\left(\frac{\varepsilon^*}{\varepsilon_{os}}\right)^{n_s}\alpha_s\exp\left(\frac{-Q_s}{RT}\right) \quad (3)$$

from the above equation, it is clear that the stress relaxation rate of closed-cell foams also depends on their relative density, the imposed strain and the stress relaxation parameters of solid material from which they are made. By setting ϕ=1, Eq. (3) reduces to the result of Eq. (2) for open-cell foams.

In real closed-cell foams, such as foamed high-alumina cement paste we studied here, their cell geometry is different from that assumed in the theoretical cell-edge relaxation-bending model of Lin and Huang [7]. That is, the cell geometry of spherical cells within foamed cement paste cannot be modeled thoroughly by using the cubic model of Fig. 1. Nevertheless, the cell-edge relaxation-bending model is still the primary deformation mechanism for the stress relaxation of foamed cement paste. It can be expected that the stress relaxation rates of foamed cement pastes are affected by their relative density, the imposed strain and the activation energy of solid cement paste. As a result of that, a theoretical expression for describing the stress relaxation rate of foamed cement paste can be obtained by accounting for the difference of cell geometry between the theoretical cell-edge relaxation-bending model and the real microstructure of foamed cement paste:

$$\dot{\sigma}^* = \left[C_3\left(\frac{\rho^*}{\rho_s}\right)^{(n_s+3)/2} + C_4\left(\frac{\rho^*}{\rho_s}\right)\right]\left(\frac{\varepsilon^*}{\varepsilon_{os}}\right)^{n_s}\exp\left(\frac{-Q_s}{RT}\right) \quad (4)$$

wherein the two microstructural coefficients C_3 and C_4 should be determined from experimental results.

3. Experimental methods

The constituents for producing foamed cement paste specimens are high-alumina cement, water, superplasticizer and preformed air bubbles. Foamed cement paste with a water/cement ratio of 0.6 and adequate amount of superplasticizer was made to ensure a good workability for placing them into cylindrical moulds. The dosage of superplasticizer is 0.5% of total cement weight to reduce the water/cement ratio of the mix. The preformed air bubbles were made by pressuring an aqueous solution of a foaming agent (manufactured by Elastizell Corporation of America, Ann Arbor, MI, USA) diluted with water in a foam generating tank. The density of foamed high-alumina cement paste is controlled by changing the amount of preformed air bubbles poured into slurry of high-alumina cement paste. The required amount of each constituent for producing foamed high-alumina cement paste with different densities was calculated and weighed before mixing. After complete mixing of high-alumina cement paste and preformed air bubbles, foamed high-alumina cement paste was placed into cylindrical PVC moulds with an inner diameter of 55 mm and a height of 250 mm. One day later, the foamed high-alumina cement paste specimens were removed from the cylindrical PVC moulds and cured at ambient room temperature in water for 28 days. Before mechanical testing, the foamed high-alumina cement paste specimens were trimmed on both ends and then air-dried for additional 7 days.

A series of stress relaxation tests on foamed high-alumina cement paste were conducted to verify the applicability of the theoretical expression proposed for describing the stress relaxation rates of closed-cell foams. At first, the stress relaxation rates of foamed high-alumina cement pastes with various relative densities under different imposed strains but at the same temperature were measured to evaluate the dependences of stress relaxation rates on relative density and imposed strain. The temperature was fixed at T=35 °C, while four different imposed strains ε^*=0.006, 0.008, 0.01 and 0.012 were considered for the stress relaxation rates of foamed high-alumina cement pastes with various relative densities; the relative densities of foamed high-alumina cement pastes were 0.2, 0.3, 0.4 and 0.5. Then, the stress relaxation rates of foamed high-alumina cement pastes under different temperatures but at the same

imposed strain ε^*=0.008 were measured to determine the activation energy for the stress relaxation process; the temperatures considered here were T=35, 55, 75 and 95 °C.

The temperature of the chamber used for measuring the stress relaxation rates of foamed high-alumina cement pastes can be controlled in the range of 25 to 250 °C. Before stress relaxation testing, the chamber was first heated up to the desired temperature. Then, a foamed high-alumina cement paste specimen was put in the chamber for 3 h to ensure that the whole specimen reaches the desired temperature. The upper fixture plate was moved slowly to contact the specimen surface. A fixed strain was imposed on the specimen, and the corresponding stress at any instant was monitored by a personal computer. Experimental results were recorded up to 200 min to determine the corresponding stress relaxation rate for each foamed high-alumina cement paste specimen.

The rate of stress relaxation or creep of cement paste depends on the loading time and the imposed strain or stress. In many cases, the rate of stress relaxation or creep can be described approximately by an exponential, hyperbolic or logarithmic function. For foamed cement paste that we studied here, the rate of stress relaxation presumably will be affected by the loading time, the relative density of foamed cement paste and the imposed strain. In the paper, we aim at analyzing the dependences of stress relaxation rates of foamed high-alumina cement pastes at any instant on their relative density and the imposed strain. Therefore, the stress relaxation rates after 60 min of loading for foamed high-alumina cement pastes with different relative densities subjected to various imposed strains were measured.

4. Results and discussion

The micrographs of foamed high-alumina cement paste with a relative density of 0.2 and 0.5 are shown in Figs. 3 and 4, respectively. It is seen that the thicknesses of cell edges and cell faces become thicker as the relative density of foamed high-alumina cement paste is increased. However, the cell sizes are roughly the same, regardless of their relative density; the mean cell sizes are 249.7, 240.0, 235.1 and 228.3 μm for foamed high-alumina cement pastes with a relative density of 0.2, 0.3, 0.4 and 0.5, respectively. The measured stress relaxation rates of foamed high-alumina cement pastes under the same temperature T=35 °C are plotted against the imposed strains ε^*=0.006, 0.008, 0.01 and 0.012, as shown in Fig. 5. From Fig. 5, it is found that the stress relaxation rates of foamed high-alumina cement pastes increase with the imposed strains. The reason is that the bending moment and deformation of solid cell walls are larger when a larger fixed strain is imposed on foamed high-alumina cement pastes, resulting in a higher stress relaxation rate; time-dependent deformation of solid cell walls was found to be responsible for the time-dependent behavior of foamed materials [9–12]. From Eq. (4), it is also known that

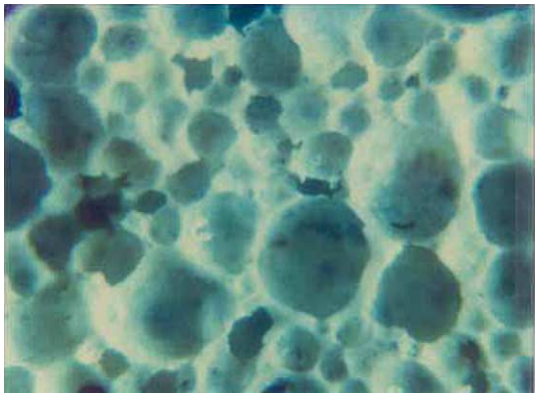

Fig. 3. The micrograph of a foamed high-alumina cement paste with a relative density of 0.2.

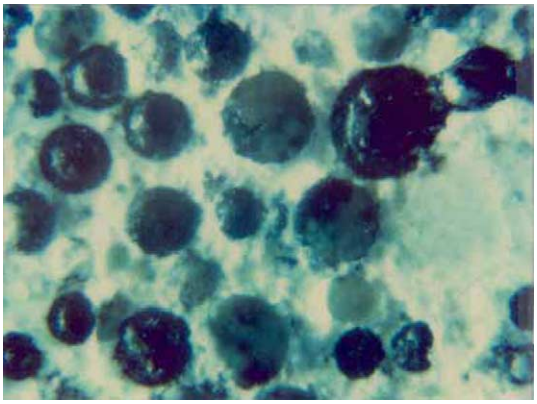

Fig. 4. The micrograph of a foamed high-alumina cement paste with a relative density of 0.5.

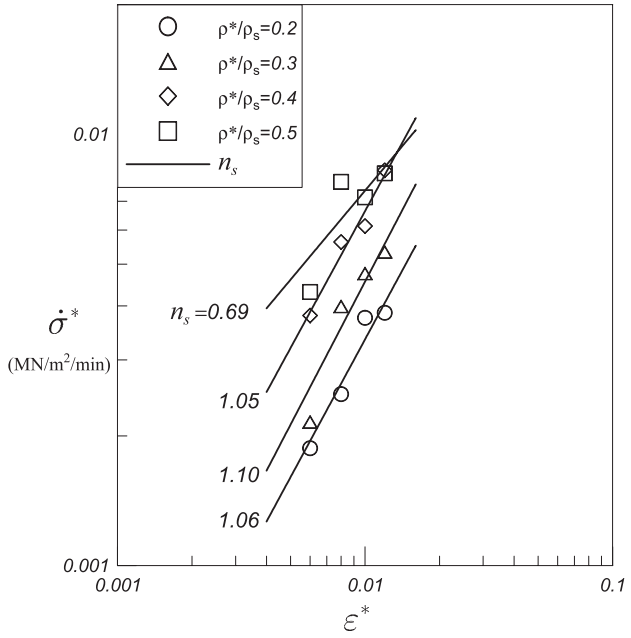

Fig. 5. The stress relaxation rates of foamed high-alumina cement pastes with various relative densities under the same temperature T=35 °C are plotted against their imposed strains, giving the stress relaxation parameter n_s.

the stress relaxation rates of foamed cement pastes depend on the imposed strain with an exponent constant of n_s. Experimental results on the stress relaxation rates of foamed high-alumina cement pastes subjected to different imposed strains, as shown in Fig. 5, suggest that n_s=1.06 (linear regression, R^2=0.92) when ρ^*/ρ_s=0.2, n_s=1.1 (R^2=0.92) when ρ^*/ρ_s=0.3, n_s=1.05 (R^2=0.95) when ρ^*/ρ_s=0.4 and n_s=0.69 (R^2=0.67) when ρ^*/ρ_s=0.5; the mean value of the measured exponent constants is 0.975. It is noted that the measured exponent constant for foamed high-alumina cement paste with a relative density of 0.5 is slightly low. The reason that is that the foamed high-alumina cement paste with a relative density of 0.5 is closer to a porous solid instead of a foamed material. Hence, the stress relaxation rate of foamed high-alumina cement paste with a higher relative density cannot be described well by the theoretical expression of Eq. (4) derived from the cell-edge relaxation-bending model.

From Fig. 5, it is also seen that the stress relaxation rates of foamed high-alumina cement pastes increase with their relative density when they are subjected to the same imposed strain. Since the thicknesses of solid cell edges and cell faces are thicker for foamed high-alumina cement paste with a higher relative density, the required forces and moments exerted on solid cell edges and cell faces to produce the same deflection are higher. As a result of that, the time-dependent deformation of solid cell edges and cell faces will be more significant, giving a higher stress relaxation rate.

By setting n_s=0.975 in Eq. (4), the theoretical expression for describing the stress relaxation rates of foamed high-alumina cement pastes we studied becomes:

$$\dot{\sigma}^* = \left[C_3\left(\frac{\rho^*}{\rho_s}\right)^{1.988} + C_4\left(\frac{\rho^*}{\rho_s}\right)\right]\left(\frac{\varepsilon^*}{\varepsilon_{os}}\right)^{0.975}\exp\left(\frac{-Q_s}{RT}\right) \tag{5}$$

to evaluate the effect of relative density on the stress relaxation rates of foamed high-alumina cement pastes, Eq. (5) can be rearranged as:

$$\frac{\dot{\sigma}^*}{\varepsilon^{*0.975}} = \left[C_3\left(\frac{\rho^*}{\rho_s}\right)^{1.988} + C_4\left(\frac{\rho^*}{\rho_s}\right)\right]\frac{\exp(-Q_s/RT)}{\varepsilon_{os}^{0.975}} \tag{6}$$

Hence, the ratio of $\dot{\sigma}^*/\varepsilon^{*0.975}$ for each foamed high-alumina cement paste specimen is plotted against its relative density as shown in Fig. 6. In Fig. 6, experimental results on the stress relaxation rates of foamed high-alumina cement pastes with different relative densities are compared to Eq. (4) when n_s=0.975, C_3=0.7, C_4=1.25 and $\exp(-Q_s/RT)/\varepsilon_{os}^{0.975}$=4 MN/m^2/min; the agreement is good. Therefore, it can be said that the stress relaxation rates of foamed high-alumina cement pastes subjected to the same imposed strain increase nonlinearly as their relative density is increased.

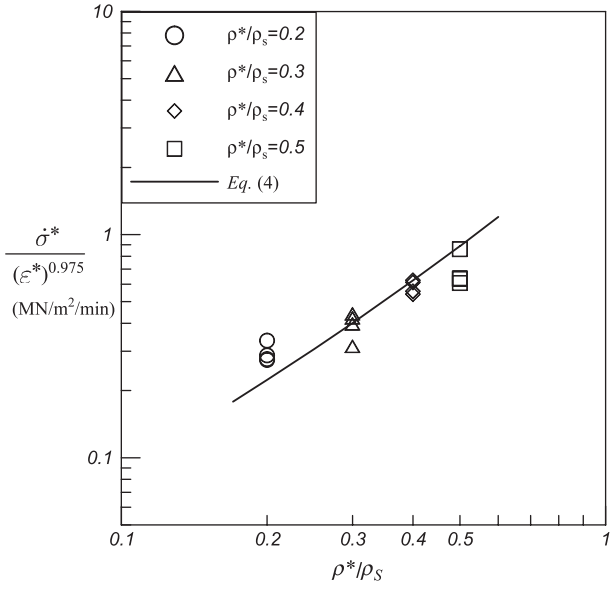

Fig. 6. The dependence of $\dot{\sigma}^*/\varepsilon^{*0.975}$ on ρ^*/ρ_s for foamed high-alumina cement pastes with various relative densities and under different imposed strains.

The elastic moduli are 0.30, 0.67, 1.02 and 1.58 GPa for foamed alumina cement pastes with a relative density of 0.2, 0.3, 0.4 and 0.5, respectively. When the maximum strain ε^*=0.012 is imposed on the foamed alumina cement pastes, the induced macroscopic stresses are 3.6, 8.0, 12.2 and 18.9 MPa for foamed alumina cement pastes with a relative density of 0.2, 0.3, 0.4 and 0.5, respectively. Since the macroscopic stresses are carried by solid cell walls, the locally acting stress of solid cell walls σ_s can be roughly estimated from the macroscopic stresses σ^* through the relationship of $\sigma^*=\sigma_s(\rho^*/\rho_s)$. The locally acting stresses of solid cell walls are found to be 18, 26.7, 30.5 and 37.8 MPa for the foamed cement pastes we studied here. Therefore, the stress relaxation rates of foamed cement pastes with a higher relative density are larger when they are subjected to the same imposed strain.

In addition, the stress relaxation rates of foamed high-alumina cement pastes are affected by their service temperature. By setting n_s=0.975 in Eq. (4), the following relationship can be obtained:

$$\ell n(\dot{\sigma}^*) = \ell n\left\{\left[C_3\left(\frac{\rho^*}{\rho_s}\right)^{1.988} + C_4\left(\frac{\rho^*}{\rho_s}\right)\right]\right\} + 0.975\ell n\left(\frac{\varepsilon^*}{\varepsilon_{os}}\right) - \frac{Q_s}{RT} \tag{7}$$

when the stress relaxation rates of foamed high-alumina cement pastes $\dot{\sigma}_T^*$ at temperatures T=55, 75 and 95 °C are divided by the stress relaxation rates of foamed high-alumina cement pastes $\dot{\sigma}_{T_0}^*$ at temperature T_0=35 °C, then the following relationship can be obtained from Eq. (7):

$$\ell n\left(\frac{\dot{\sigma}_{T_0}^*}{\dot{\sigma}_T^*}\right) = -\frac{Q_s}{R}\left(\frac{1}{T_0} - \frac{1}{T}\right) \tag{8}$$

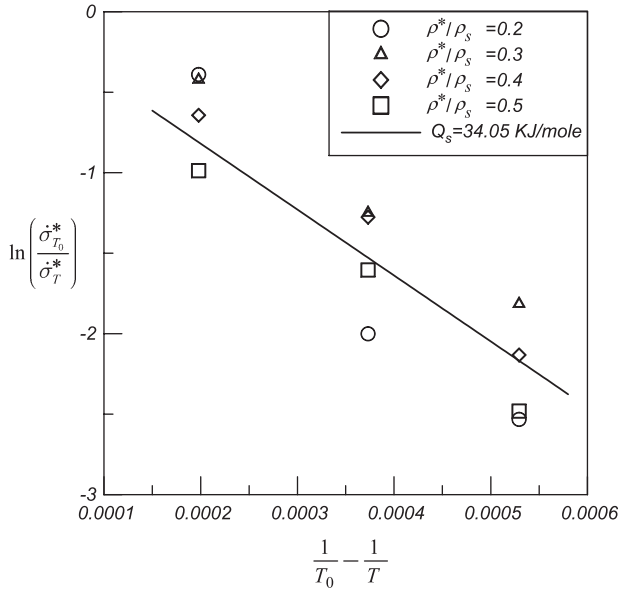

Fig. 7. The normalized stress relaxation rates $\dot{\sigma}^{*}_{T_0}/\sigma^{*}_{T}$ are plotted against $1/T_0-1/T$ to determine the activation energy for stress relaxation of foamed high-alumina cement paste.

The normalized stress relaxation rates $\dot{\sigma}^{*}_{T_0}/\dot{\sigma}^{*}_{T}$ calculated from experimental results of foamed high-alumina cement pastes with various relative densities under the same imposed strain ε^{*}=0.008 but different temperatures are plotted against $1/T_0$–$1/T$, as shown in Fig. 7. Since the ideal gas constant R=8.314 J/mol^{0}K is known, the activation energy of stress relaxation Q_s for foamed high-alumina cement pastes can be found by comparing experimental results to Eq. (8). The activation energies for foamed high-alumina cement pastes with a relative density of 0.2, 0.3, 0.4 and 0.5 can be determined from Fig. 7 and are found to be 39.23, 27.37, 31.4 and 38.2 KJ/mol, respectively; the mean activation energy for foamed high-alumina cement pastes we studied is approximately 34.05 KJ/mol. The activation energies obtained here are within the range (from 20 to 120 KJ/mol) for stress relaxation of solid cement pastes [13–15].

By substituting the mean values n_s=0.975, Q_s=34.05 KJ/mol, C_3=0.7 and C_4=1.25 determined from experimental results into Eq. (4), the theoretical expression for describing the stress relaxation rates of foamed high-alumina cement pastes becomes:

$$\dot{\sigma}^{*}=\left[0.7\left(\frac{\rho^{*}}{\rho_s}\right)^{1.988}+1.25\left(\frac{\rho^{*}}{\rho_s}\right)\right]\left(\frac{\varepsilon^{*}}{\varepsilon_{os}}\right)^{0.975}\times\exp\left(\frac{-34.05\ \mathrm{KJ/mol}}{RT}\right) \quad (9)$$

therefore, it can be said that the stress relaxation rate of any foamed high-alumina cement paste can be estimated from Eq. (9) once its relative density and the imposed strain are known.

5. Conclusions

A theoretical expression for describing the stress relaxation rates of foamed cement pastes is obtained from a cell-edge relaxation-bending model. Theoretical result indicates that the stress relaxation rates of closed-cell foamed cement pastes depend on their relative density, the imposed strain and the stress relaxation parameters of solid cement pastes. The stress relaxation rates of foamed high-alumina cement pastes with various relative densities under different imposed strains and temperatures are measured and then compared to the theoretical expression. It is found that the stress relaxation parameter of solid high-alumina cement pastes n_s=0.975, indicating that the stress relaxation rates of foamed high-alumina cement pastes increase almost linearly with the imposed strain but increase nonlinearly with their relative density. Meanwhile, the mean activation energy for stress relaxation of foamed high-alumina cement pastes Q_s=34.05 KJ/mol is obtained from experimental results. As a result, the theoretical expression for describing the stress relaxation rates of foamed high-alumina cement pastes is found. Therefore, the stress relaxation rates of foamed high-alumina cement pastes can be estimated from the theoretical expression we proposed if their relative density and imposed strain are known.

Acknowledgement

The financial support of the National Science Council, Taiwan, Republic of China under contract number NSC 91-2211-E006-067 is gratefully acknowledged. Comments and suggestions given by reviewers are highly appreciated.

References

[1] J.M. Davies, Lightweight Sandwich Construction, Blackwell Science, Oxford, UK, 2001.
[2] L.J. Gibson, M.F. Ashby, Cellular Solids: Structure and Properties, 2nd ed., Cambridge University Press, Cambridge, UK, 1997.
[3] A. Short, W. Kinniburgh, Lightweight Concrete, 3rd ed., Applied Science, London, UK, 1978.
[4] J.S. Huang, Z.H. Huang, Fatigue of cement foams in axial compression, J. Mater. Sci. 35 (2000) 4385–4391.
[5] J.S. Huang, K.D. Liu, Mechanical properties of cement foams in shear, J. Mater. Sci. 36 (2001) 771–777.
[6] J.S. Huang, C.K. Cheng, Fracture toughness variability of foamed alumina cements, Cem. Concr. Res. 34 (5) (2004) 883–888.
[7] J.Y. Lin, J.S. Huang, Stress relaxation of cellular materials, J. Compos. Mater. (2004) (in press).
[8] V.A. Lapsa, Stress relaxation phenomena at early technological phases of gas-concrete, ACI Mater. J. 96 (1999) 436–439.
[9] J.S. Huang, L.J. Gibson, Creep of polymer foams, J. Mater. Sci. 26 (1991) 637–647.
[10] K.C. Goretta, R. Brezny, C.Q. Dam, D.J. Green, A.R. De Arellano-Lopez, A. Dominguez-Rodriguez, High temperature mechanical behavior of porous open-cell Al_2O_3, Mater. Sci. Eng., A Struct. Mater.: Prop. Microstruct. Process. A124 (1990) 151–158.

[11] E.W. Andrews, J.S. Huang, L.J. Gibson, Creep behavior of a closed-cell aluminum foam, Acta Mater. 47 (1999) 2927–2935.
[12] E.W. Andrews, L.J. Gibson, M.F. Ashby, The creep of cellular solids, Acta Mater. 47 (1999) 2853–2863.
[13] F.H. Wittman, Hydraulic Cement Pastes: Their Structure and Properties, Cement and Concrete Assoc, Slough, UK, 1976.
[14] R.L. Day, B.R. Gamble, The effect of changes in structure on the activation energy for the creep of concrete, Cem. Concr. Res. 13 (1983) 529–540.
[15] W.P.S. Dias, G.A. Khoury, P.J.E. Suillivan, An activation energy approach for the temperature dependence of basic creep of hardened cement paste, Mag. Concr. Res. 39 (1987) 141–147.